



UNIVERSITEIT•STELLENBOSCH•UNIVERSITY
jou kennisvenoot • your knowledge partner

*Design and optimisation of a line-start synchronous reluctance motor
(repository copy)*

Article:

Smit, Q., Sorgdrager, A. J., Wang, R.-J., (2016) Design and optimisation of a line-start synchronous reluctance motor, *Proc. of the Southern African Universities Power Engineering Conference*, (SAUPEC), Johannesburg, South Africa, 26-28 January 2016

<http://dx.doi.org/10.13140/RG.2.1.4266.8560>

Reuse

Unless indicated otherwise, full text items are protected by copyright with all rights reserved. Archived content may only be used for academic research.

DESIGN AND OPTIMISATION OF A LINE-START SYNCHRONOUS RELUCTANCE MOTOR

Q. Smit*, A.J. Sorgdrager** and R-J. Wang**

* Stellenbosch University, Department of Mechanical and Mechatronic Engineering, Corner of Bosman Road and Victoria Street, Stellenbosch 7600, South Africa

Email: 16139844@sun.ac.za

** Stellenbosch University, Department of Electrical and Electronic Engineering, Corner of Bosman Road and Victoria Street, Stellenbosch 7600, South Africa

Email: ajsorgdrager@gmail.com; rwang@sun.ac.za

Abstract: In this study a line-start reluctance synchronous machine (LS-SynRM) was designed and optimised using a finite element method based approach. Simulation results showed that the optimised LS-SynRM when compared to an induction machine achieved better efficiency, but lower power factor and higher torque ripple. Based on the simulation results, a LS-SynRM prototype was manufactured and experimentally tested. The prototype did however not achieve synchronization under loaded conditions. Possible causes were discussed and relevant conclusions are drawn.

Keywords: Line-start motor, reluctance synchronous machine, induction machine, synchronisation, design optimisation, transient performance.

1. INTRODUCTION

As of 2013, rotating electrical machines consume 40% of global electrical energy and 70% in industry applications [1]. This resulted in energy efficiency with regards to rotating electrical receiving a considerable amount of attention in recent years. With the advent of IEC 60034-30 standard, there has been a big drive in electrical machine industry to look into alternative machine technologies that could meet with the forthcoming IE4 efficiency standard. Since synchronous machines tend to have better efficiencies than their asynchronous counterparts, the industry has seen a gradual shift towards synchronous operating machines.

Synchronous machines typically are not line-start machines and require expensive power inverter control systems for start-up. Conversely, induction machines can start simply by connecting to a constant frequency line-voltage. Line-start synchronous machines attempt to remove the weakness of synchronous machines by creating a hybrid motor that has high efficiency at steady-state operation and the ability to self-start. Different line-start electrical machine technologies have been proposed in literature. Amongst others, line-start synchronous reluctance machines (LS-SynRM) have received some attention [2-3].

In this paper, the design process and practical evaluation of a LS-SynRM including rotor concept selection, FEM based design optimisation, prototype construction and finally experimental testing are presented. The intended application of this machine is for fans and pumps loads operate for long periods of time at a constant speed.

2. CONCEPT DEVELOPMENT AND SELECTION

For this study a standard WEG 2.2kW 525V 4-pole three-phase premium efficiency cage induction motor (IM) is used as a reference motor. An LS-SynRM can utilize the

same winding configuration and design as an IM, thus the stator configuration of the reference IM is used for all LS-SynRM designs in the study. Figures 1 and 2 present the stator winding layout and the rotor design of the IM respectively.

For the LS-SynRM rotor design, three different concepts are considered. Concept 1 (Fig. 3) uses the existing squirrel cage structure of the reference IM as in Fig.2 with an internal flux barrier structure. Concept 2 (Fig. 4) has a typical flux barrier structure surrounded by a solid copper sleeve. Concept 3 (Fig. 5) adopts a complete SynRM rotor and simply inserts the cage conductors into the available spaces inside the flux barriers.

2.1 FEM Model

To evaluate the design concepts, two-dimensional (2D) finite element analyses (FEA) were conducted by using ANSYS' Maxwell v16 software package and the motor design toolkit plug-in. The software employs time-stepped transient FE simulation to determine the transient

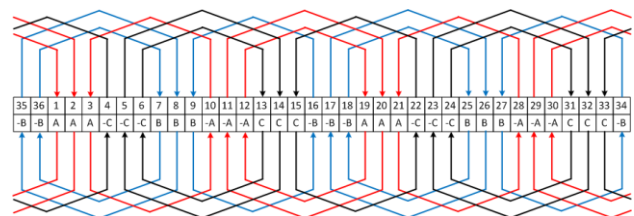


Figure 1: IM stator winding layout

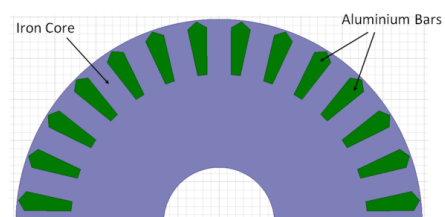


Figure 2: Reference induction machine rotor

synchronisation response and steady-state performances of electrical machines using the toolkit.

Considering the geometrical symmetry of the machine, it is necessary to model only one half of the machine by applying a positive periodical boundary condition. Assuming the magnetic field is fully contained within the stator, the magnetic vector potential along the outer surface of the stator is defined as 0 Wb.m^{-1} , which is the so-called Dirichlet boundary condition. The FE model of a LS-SynRM is shown in Fig. 6.

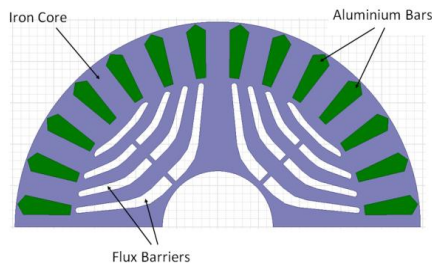


Figure 3: Rotor design concept 1

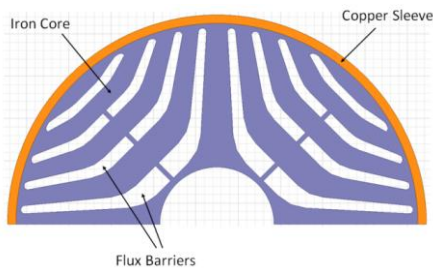


Figure 4: Rotor design concept 2

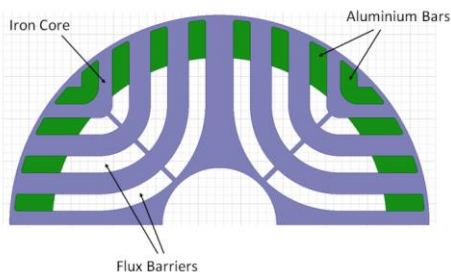


Figure 5: Rotor design concept 3

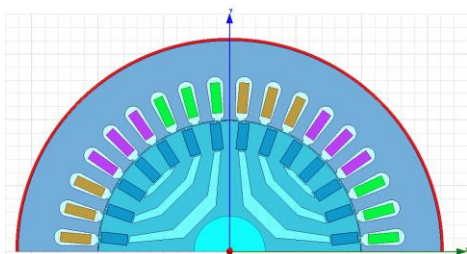


Figure 6: LS-SynRM's FEA model

2.2 Rotor Concept Selection

From the initial non optimized design analyses results as presented in Table 1, it appears that Concept 3 has the best steady-state performances. However, it requires unrealistically low conductivities in both cage conductor bars and the end rings in order to achieve synchronisation. The resulting end ring thickness and

conductor bar cross sections are not practically realisable, and therefore Concept 3 was excluded from the selection.

Concepts 1 and 2 both show good synchronisation ability. Concept 1 demonstrates better efficiency and power factor than Concept 2, while Concept 2 has lower torque ripple (Table 1). Concept 1 was selected for further design optimisation, since existing design techniques can be applied in the design of LS-SynRM to reduce the torque ripple [4-5].

Table 1: Performance comparison of different concepts

Rotor concept	1	2	3
Synchronisation	Yes	Yes	No
Efficiency (%)	87.3%	53.5%	95.1%
Power Factor	0.58	0.49	0.79
Torque ripple (%)	33.8%	5.9%	14.3%

3. CONCEPT REVISION AND DESIGN SPACE

The selected concept was further revised by changing the conductor bar cross section into a rectangular shape which allows for the insertion of standard aluminium flat bar instead of casting. Additionally, the number of flux barriers is reduced to three per pole which corresponds to the optimum number for torque ripple minimisation as proposed by Vagati [4-5].

Conductor slot openings are also added to give additional control over the torque ripple. After defining constraints, a total of 6 design variables (as shown in Fig. 7) remained to define the design space, of which 3 variables are required for defining the flux barrier size and width; 2 variables are needed to characterise the conductor bar cross section and a single variable defines the width of the conductor slot opening.

4. OPTIMISATION

As shown in Fig. 8, the optimisation was conducted in 3 sequential steps. Firstly, the conductor bar cross section was determined by selected the minimum cross section that could still successfully synchronise (with a safety factor of 50%). Cross sections were selected from a supplier's aluminium flat bar catalogue. Secondly, the flux barrier variables were optimised for efficiency and power factor using a full parametric sweep. Finally the conductor slot opening width was optimised to reduce torque ripple and further increase efficiency.

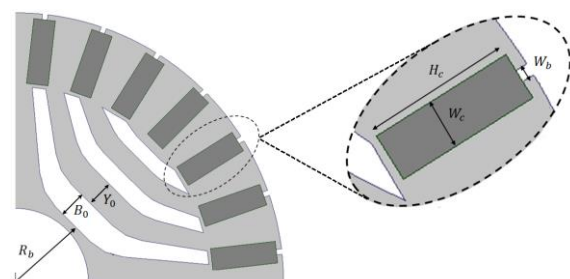


Figure 7: Optimisation design space showing 6 variables

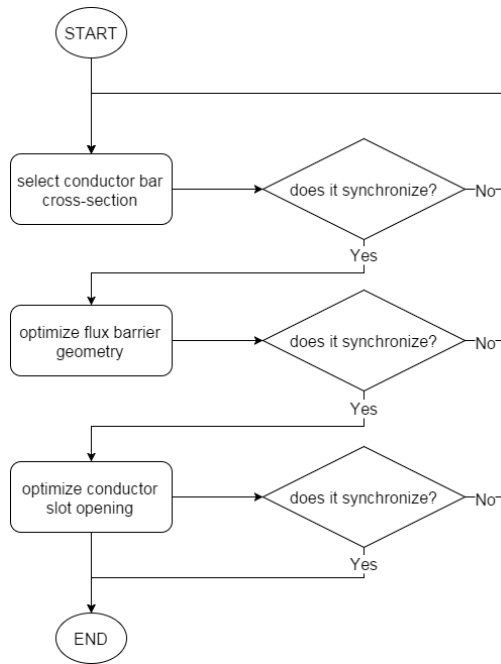


Figure 8: Optimisation design flow chart

4.1 Flux barrier optimisation

Table 2 shows the best performing flux barrier parametric sweep results ranked in terms of efficiency. Even though there are large differences in the geometry variables, the efficiency results are within $\pm 0.1\%$ of each other. The results with higher efficiencies also correspond to higher power factors and lower stator currents. This can be explained by the fact that; for LS-SynRM, the highest losses occur due to the I^2R losses of the stator windings and are therefore directly linked to the stator current.

The second ranked design is chosen as it has a larger bottom flux barrier radius (R_b), which corresponds to thicker and stronger ribs between the shaft and the bottom flux barrier. Additionally, the second ranked variation also has lower torque ripple.

4.2 Conductor slot opening optimisation

To select the slot opening width a parametric sweep was done to investigate the effects it has on both the rms line current and the torque ripple. The simulation results are presented by Fig 9. The point at which the supply current is the lowest (as indicated on the plot) is selected as the optimum width, this also corresponds to a relatively low torque ripple.

Table 2: Flux barrier geometry optimisation

	Geometry (mm)			Performance			
	B_0	R_b	Y_0	TR (%)	Eff. (%)	Phase Current (Arms)	PF
1	6	15	7	36.1	93.88	2.44	0.74
2	5	16	7	31.0	93.85	2.44	0.74
3	7	14	7	31.8	93.81	2.45	0.74
4	6	14	8	33.2	93.79	2.45	0.74
5	6	16	6	33.6	93.78	2.46	0.74

4.3 Geometry comparison

Fig. 10 compares the initial rotor geometry with the optimised rotor geometry. It can be seen that the optimised result favours a structure with almost perfect flux barrier alignment with the conductor bars. This is an intuitive result, since the conductor bars should essentially become extensions of the flux barriers due to the magnetic saturation of the webs between them resulting in improved reluctance torque and steady state performance.

4.4 Optimisation results

Table 3 shows the effectiveness of the optimisation process by comparing the performance of the optimised geometry with the initial unoptimised geometry and the simulated reference induction motor.

Table 3: Optimisation performance comparison

Performance	Initial	Optimised	Induction motor
Efficiency	92.46 %	93.69 %	92.95 %
Power factor	0.615	0.656	0.693
Torque ripple	29.6 %	29.9 %	18.7 %

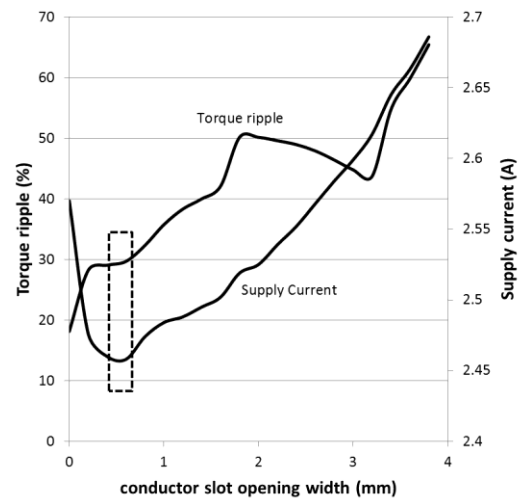
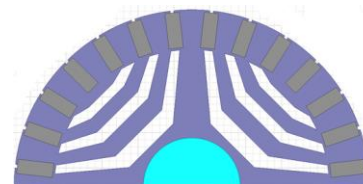
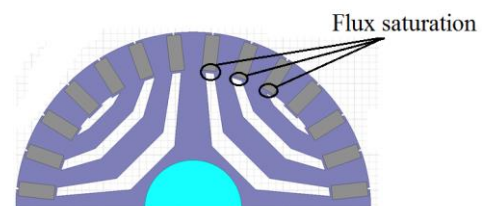


Figure 9: Effect of conductor slot opening width



(a) unoptimised design



(b) optimised design

Figure 10: Design geometry comparison

The optimisation process improved efficiency by more than 1% over the original geometry. Additionally, the efficiency is more than 0.7% better when compared to the simulated induction motor. The power factor and torque ripple of the optimised geometry is still worse than the reference IM, indicating that the LS-SynRM is only preferable in high efficiency applications where torque ripple and power factor are not a major consideration.

5. MANUFACTURING OF A PROTOTYPE

The optimised geometry was laser-cut using M400-50A electrical steel as shown in Fig. 11. The close-ups show that the quality of the laser cutting was relatively poor.

Figure 12 presents the manufacturing steps taken. The laminations were stacked onto a dummy shaft with the aluminium conductors positioned inside the conductor slots (Fig 12a). The end rings were pressed onto both sides of the rotor to secure the lamination stack (Fig 12b). A stacking factor of 0.95 is achieved for the 120 mm shaft. The end rings were then TIG welded using aluminium filler in order to improve the cage conductivity and overall rotor strength (Fig 12c). The dummy shaft was removed after which the machined shaft was inserted to ensure compatibility with the IM stator. Finally, compatible NHK bearing and keyways were fitted with the final rotor as presented in Fig 12d.

6. EXPERIMENTAL RESULTS

In this section the testing setup and results are described. Fig. 13 shows the test setup used for the prototype LS-SynRM.

A Norma 3000 power analyser is connected in series with all three lines of the input power supply using shunt resistors. This power analyser can measure the steady-state electrical input power and power factor very accurately; however it is unable to take transient measurements required during transient performance of the machine. The transient voltages and currents are measured using a TiePie Handy-Scope HS4 DIFF digital oscilloscope, which is connected to a PC via USB where they are interpreted by a software suite. The DR-3000 digital torque sensor is connected to the shaft and fan load with spider couplings. The torque sensor is connected to a PC via USB and results are interpreted by a software suite. The torque sensor is capable of taking transient or steady-state shaft torque, speed and output power readings.

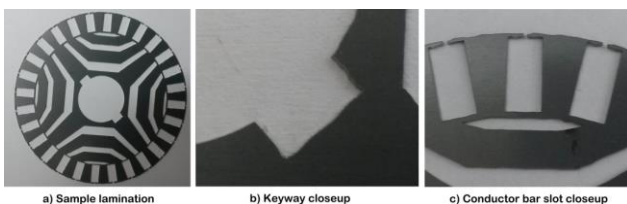


Figure 11: Rotor lamination

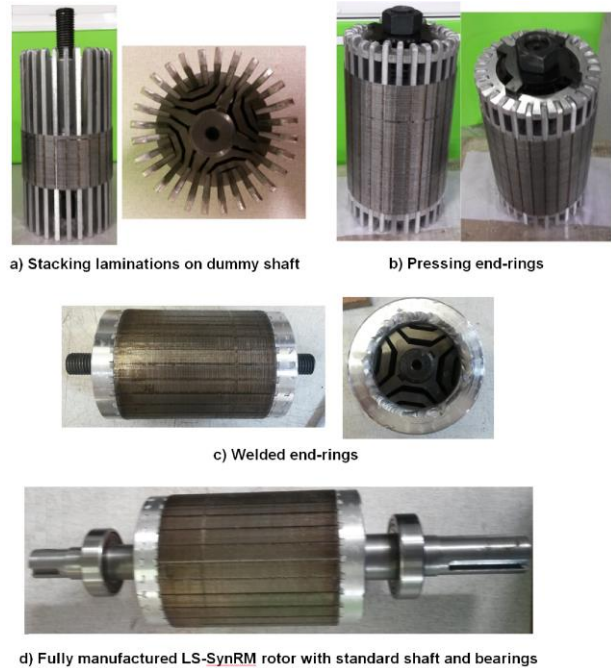


Figure 12: Manufacturing process for LS-SynRM rotor

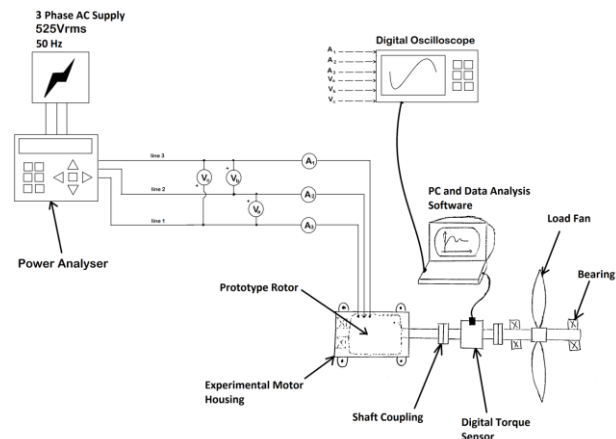


Figure 13: Experimental setup

Figure 14 shows the measured speed versus time characteristics of the LS-SynRM under no-load and full load conditions. The prototype motor was able to synchronise under the no-load condition, but was unable to synchronise while driving the fan load.

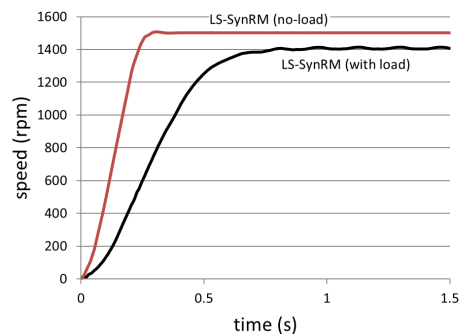


Figure 14: Measured speed versus time characteristics of the prototype LS-SynRM machine

7. ANALYSIS OF SYNCHRONISATION FAILURE

Since the prototype machine failed to synchronise contrary to the simulation prediction, further analysis on the possible causes was conducted. Considering the large effect of inertia on synchronisation, some evidence regarding its influence was investigated. The graph in Fig. 15 compares the measured speed versus time starting response of the induction motor with the simulated ones at different load inertia assumptions. The simulated response at the initial inertia assumption 0.11 kg.m^2 does not match the measured response well. However, if the inertia assumption is increased from the initial 0.11 to 0.17 kg.m^2 , the simulated response matches the measured response very well. This implies that the actual inertia of the load could be higher than the original assumption used in the design.

The graph in Fig. 16 shows the simulated speed versus time starting response of the LS-SynRM at various system inertia values. Clearly, the motor fails to synchronise with system inertia of 0.17 kg.m^2 , however at the slightly lower inertia of 0.16 kg.m^2 the motor can still synchronise. This result indicates the actual system inertia maybe be just outside synchronisation capability of the prototype machine.

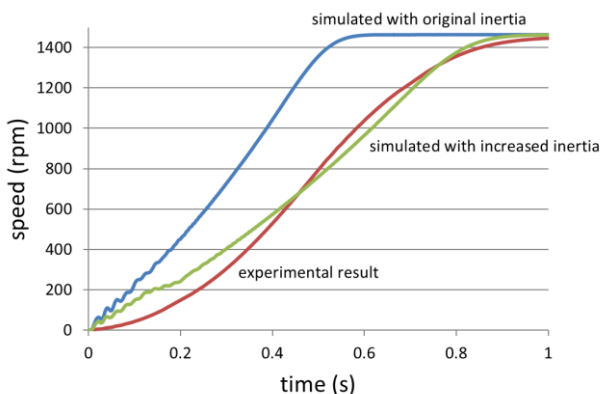


Figure 15: IM inertia comparison

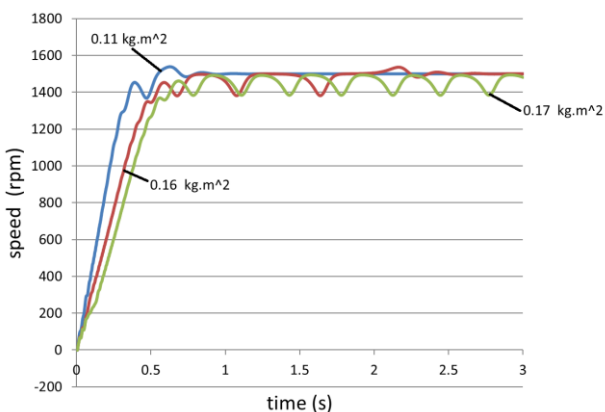


Figure 16: Simulated LS-SynRM at various inertias

8. CONCLUSION

Even though the prototype failed to synchronise, the most likely cause was determined to be the underestimation of load inertia. The FEM optimisation results showed that better efficiency than a typical induction machine can be achieved; however the power factor and torque ripple may still be inferior. The LS-SynRM should thus only be considered in high efficiency applications where power factor and torque ripple are not a major concern.

From a manufacturing perspective, the costs of LS-SynRMs should be similar to IMs as practically the same manufacturing process can be followed. This is a major advantage over other line-start alternatives such as the line-start permanent magnet machine which is generally more expensive than typical IMs.

9. RECOMMENDATIONS

In light of the failed synchronisation, recommendations are made with regard to future work. Firstly, the motor can be redesigned using the new inertia assumption by following the same process laid out in this paper. Secondly, the test load can be modified to reduce the inertia so synchronisation is achieved.

Once a synchronising is achieved, the effect of inserting magnets along the q -axis should be investigated as this could improve steady state performance without deteriorating synchronisation and torque ripple. The prototype's flux barriers were designed to ensure compatibility with rectangular magnets.

REFERENCES

- [1] J. Estima and A. Cardoso: "Efficiency Analysis of Synchronous Reluctance Motors." *International Conference on Engineering*. UBI2013. Nov 2013.
- [2] S.T. Boroujeni, N. Bianchi and L. Alberti: "Fast estimation of line-start reluctance machine parameters by finite element analysis," *IEEE Trans. Energy Convers.*, Vol. 26, No. 1, pp. 1–8, March 2011.
- [3] S.T. Boroujeni, M. Haghparast and N. Bianchi: "Optimization of Flux Barriers of Line-start Synchronous Reluctance Motors for Transient- and Steady-state Operation", *Electric Power Components and Systems*, 43:5, 594-606, 2015.
- [4] A. Vagati, G. Franceschini, I. Marongiu and G.P. Troglia: "Design criteria of high performance synchronous reluctance motors", *Industry Applications Society Annual Meeting, Conference Record of the 1992 IEEE*, vol. 1, pp. 66-73, October 1992.
- [5] A. Vagati, M. Pastorelli, G. Franceschini and S.C. Petrache: "Design of low-torque-ripple synchronous reluctance motors", *IEEE Industry Applications Society Annual Meeting*, Vol. 34, No. 4, pp. 758-765, July-August 1998.